$K(VO)(SeO_3)_2H$: A New One-Dimensional Compound with Strong Hydrogen Bonding

Yoon Hyun Kim, Kyu-Seok Lee, and Young-Uk Kwon*

Department of Chemistry, Sung Kyun Kwan University, Suwon, 440-746, Korea

Oc Hee Han

Korea Basic Science Institute, Taejeon, 305-333, Korea

Received May 28, 1996[⊗]

The hydrothermal synthesis, X-ray single crystal structure, magnetic properties, and solid state NMR and infrared spectroscopic data of a new compound, $K(VO)(SeO_3)_2H$, are described. $K(VO)(SeO_3)_2H$ crystallizes in the monoclinic space group $P2_1/m$ (No. 11), with $a = 7.8659(7)$ Å, $b = 10.4298(7)$ Å, $c = 4.0872(7)$ Å, $\beta = 96.45(1)°$, and $Z = 4$. The structure is described as parallel linear strands made of repeating $[(VO)(SeO_3)_2]^{2-}$ units. The chains are held together through hydrogen bondings between selenite oxygens, weak V═O···V═O bonds, and ionic bonds to the interchain K^+ ions. The hydrogen bonding in this compound shows many characteristics of the strong hydrogen bonding with a short O−O distance of 2.459(6) Å, a large down field shift of the proton NMR signal of 19 ± 1 ppm, and a low O−H absorption frequency. However, the exact position of the hydrogen atom and, thus, the nature of the hydrogen bonding in this compound is unclear. Possible models for the hydrogen atom positions are discussed based on experimental and literature data. The magnetic susceptibility data show an antiferromagnetic coupling below 19 K. The curve can be explained with a 1-D Heisenberg model for $S = {}^1/_2$ with $J/k = 13.8$ K and $g = 1.97$.

Introduction

Vanadium(IV) oxo compounds, especially those synthesized by hydrothermal reactions, are attracting much interest because of the variety of structures and the magnetic properties.[1,2] This class of materials have been found mainly from vanadium−phosphate and −phosphonate systems,[2] and some from the vanadium−selenite systems.[3−6] Interest in the selenite compounds stems from the expected structural similarity between SeO_3^{2-} ion and PO_4^{3-}/RPO_3^{2-} ions. Examples of vanadium(IV) selenites in the literature are $VOSeO_3 \cdot H_2O$,[3] AV_2SeO_7 (A = K and Rb),[4,5] and $Ba(VO)_2(SeO_3)_2(HSeO_3)_2$[6] which show dimer, one-dimensional antiferromagnetic, and no magnetic couplings, respectively. There are also $VOSeO_3$ and $VOSe_2O_5$ reported in the literature.[7,8]

During our investigation on the hydrothermal reactions of various vanadium selenite systems,[4,5,9] we have obtained a new compound $K(VO)(SeO_3)_2H$ with an 1D-chain structure. This compound exhibits a so-called strong hydrogen bonding with a short O···O distance of 2.459(6) Å.[10−13]

The strong hydrogen bonding has been the subject of many papers in enzyme kinetics,[14−16] physical organic,[12,13,17,18] and solid state crystal chemistry.[11] Such hydrogen bondings are found when the donor and acceptor atoms are closer than the sum of their van der Waals radii (<2.7 Å for O−H−O) and the difference of the pK_a values of these atoms is near zero. This type of hydrogen bonding shows many features including a low O−H absorption frequency in infrared spectra, an extreme downfield NMR shift of the hydrogen-bonded proton, and low isotope fractionation factors as well as short donor and acceptor distances from X-ray and neutron diffractions. Sometimes, the strong hydrogen bondings are divided into two types of, namely, strong (or low barrier; asymmetric) and very strong (or single well; symmetric) hydrogen bondings depending on the symmetry around the hydrogen atom and, as a consequence of the geometry, on the binding energy.[15] In both cases, the O−H−O bond angles are (nearly) 180°. Distinction between these two is not an easy task. There is no reliable spectroscopic method to address the difference of the two types of hydrogen bondings. Diffraction may be the only way. However, the X-ray diffraction method has limited validity because of its low sensitivity

[⊗] Abstract published in *Advance ACS Abstracts,* November 1, 1996.

(1) (a) Riou, D.; Ferey, G. *Inorg. Chem.* **1995**, *34*, 6520. (b) Oka, Y.; Yao, T.; Yamamoto, N. *J. Solid State Chem.* **1995**, *117*, 407. (c) Oka, Y.; Tamada, O.; Yao, T.; Yamamoto, N. *J. Solid State Chem.* **1995**, *114*, 359.
(2) (a) Bonavia, G.; Debord, J.; Haushalter, R. C.; Rose, D.; Zubieta, J. *Chem. Mater.* **1995**, *7*, 1995 and references therein. (b) Mueller, A.; Hovemeier, K.; Krickemeyer, E.; Boegge, H. *Angew. Chem., Int. Ed. Engl.* **1995**, *34*, 779. (c) Harrison, W. T. A.; Hsu, K.; Jacobson, A. J. *Chem. Mater.* **1995**, *7*, 2004. (d) Harrison, W. T. A.; Lim, S. C.; Vaughey, J. T.; Jacobson, A. J.; Goshorn, D. P.; Johnson, J. W. *J. Solid State Chem.* **1994**, *113*, 444. (e) Lii, K. H.; Wen, N. S.; Su, C. C.; Chen, B. R. *Inorg. Chem.* **1992**, *31*, 439 and references therein. (f) Haushalter, R. C.; Wang, Z.; Thomson, M. E.; Zubieta, J. *Inorg. Chem.* **1993**, *32*, 3700 and references therein.
(3) Huan, G.; Johnson, J. W.; Jacobson, A. J.; Goshorn, D. P. *Chem. Mater* **1991**, *3*, 539.
(4) Lee, K.-S.; Kwon, Y.-U.; Namgung, H.; Kim, S.-H. *Inorg. Chem.* **1995**, *34*, 4178.
(5) Kim, Y.-H.; Kwon, Y.-U. *Bull. Korean Chem. Soc.*, in press.
(6) Harrison, W. T. A.; Vaughey, J. T.; Jacobson, A. J.; Goshorn, D. P.; Johnson, J. W. *J. Solid State Chem.* **1995**, *116*, 77.
(7) Trombe, J. C.; Enjalbert, R.; Gleizes, A.; Galy, J. *C. R. Acad. Sci., Ser. 2* **1983**, *297*, 667.
(8) Trombe, J. C.; Gleizes, A.; Galy, J.; Renard, J. P.; Journaux, Y.; Verdaguer, M. *New J. Chem.* **1987**, *11*, 331.
(9) Kwon, Y.-U.; Lee, K.-S.; Kim, Y. H. *Inorg. Chem.* **1996**, *35*, 1161.
(10) Brown, I. D.; Altermatt, D. *Acta Crystallogr. B* **1985**, *41*, 244.
(11) Brown, I. D. *Acta Crystallogr. A* **1976**, *32*, 24 and references therein.
(12) Kreevoy, M. M.; Liang, T. M. *J. Am. Chem. Soc.* **1980**, *102*, 3315.
(13) Keefer, L. K.; Hrabie, J. A.; Ohannesian, L.; Flippen-Anderson, J. L.; George, C. *J. Am. Chem. Soc.* **1988**, *110*, 3701.
(14) Gerlt, J. A.; Gassman, P. G. *J. Am. Chem. Soc.* **1993**, *115*, 11552.
(15) Frey, P. A.; Whitt, S. A.; Tobin, J. B. *Science* **1994**, *264*, 1927.
(16) Schwartz, B.; Drueckhammer, D. G. *J. Am. Chem. Soc.* **1995**, *117*, 11902.
(17) Perrin, C. L.; Thoburn, J. D. *J. Am. Chem. Soc.* **1992**, *114*, 8559.
(18) Gilli, P.; Bertolasi, V.; Ferretti, V.; Gilli, G. *J. Am. Chem. Soc.* **1994**, *116*, 909.

S0020-1669(96)00624-6 CCC: $12.00

Table 1. Crystal Data and Structure Refinment for $K(VO)(SeO_3)_2H$

empirical formula: HO_7KVSe_2	space group: $P2_1/m$ (No. 11)
$a = 7.8659(7)$ Å	$T = 20(2)$ °C
$b = 10.4298(7)$ Å	$\lambda = 0.71073$ Å
$c = 4.0872(7)$ Å	$\rho_{calcd} = 3.598$ g/cm^3
$\beta = 96.450(10)°$	$\mu = 130.24$ cm^{-1}
$V = 333.19(7)$ Å^3	$R_1{}^a = 0.0222$
$Z = 4$	$wR_2{}^b = 0.0571$
fw = 180.48	

^{a} $R_1 = \sum||F_o| - |F_c||/\sum|F_o|$. ^{b} $wR_2 = [\sum|w(F_o^2 - F_c^2)^2|/\sum|w(F_o^2)^2|]^{1/2}$, $w = 1/[\rho^2(F_o^2) + (0.0218\ P)^2 + 1.22\ P]$ where $P = (F_o^2 + 2F_c^2)/3$.

to hydrogen atoms, and the neutron diffraction method cannot be utilized unless sizable single crystals are obtained.

In this paper, we report the synthesis, crystal structure, solid state NMR spectroscopic data, and magnetic properties of the novel vanadium selenite $K(VO)(SeO_3)_2H$. To our knowledge, the solid state NMR study on a proton involved in a strong hydrogen bonding has not been reported previously.

Experimental Section

Synthesis. Pure green microcrystals of $K(VO)(SeO_3)_2H$ were obtained from a hydrothermal reaction of $VOSO_4$, SeO_2, and KOH in a mole ratio of 3:15:3 (in millimoles) in 10 mL of distilled water. Single crystals of this compound were obtained when V_2O_4 was used instead of $VOSO_4$. However, the latter synthesis resulted in much lower yield and many other phases. The reactants were sealed in a Teflon-lined autoclave and heated at 230 °C for 4 days. The pH of the resultant solution was 0.7. The product solid materials were recovered by suction filtration, washing with distilled water, and air drying.

Single-Crystal X-ray Structure Analysis. A prism crystal (0.3 × 0.2 × 0.15 mm) was mounted on a glass fiber with epoxy. Crystal and intensity data of this crystal were collected on an Enraf-Nonius CAD4 diffractometer equipped with a monochromated Mo Kα (λ = 0.710 73 Å) radiation. Indexing of the 25 randomly found reflections indicated a monoclinic unit cell ($a = 7.8659(7)$ Å, $b = 10.4298(7)$ Å, $c = 4.0872(7)$ Å, $\beta = 96.45(1)°$). A data collection with a $2\theta-\omega$ mode in the θ range 2.61−24.95° was performed accordingly. The systematic extinction condition $0k0$ ($k = 2n + 1$) indicated the space groups $P2_1$ and $P2_1/m$. Both space groups were tried, and the latter was found to be the correct one. The intensity data were corrected for the time fluctuation (average 0.26% increase per hour) and Lorentz−polarization factors. An empirical ψ-scan absorption correction was applied (transmission coefficients: minimum 0.8667; maximum 0.9982; average 0.9394).

The crystal structure was solved by using the direct methods program SHELXS-86.[19] The structure refinements and difference Fourier calculations were performed with SHELXL-93[20] on F^2 data. After all non-hydrogen atoms were located and refined, the difference Fourier synthesis showed a peak with an electron density of 0.67 e$^-$/Å^3 at the 0.5, 0.5, 0.5 position, the midpoint between two symmetry related O(4) atoms that were 2.46 Å apart from each other. Although the exact position of this hydrogen is ambiguous (see Results and Discussion), this peak was assigned as a hydrogen atom and was included in the refinements for the sake of accounting for the electron density. A few cycles of the final full-matrix least-squares refinements, including the secondary extinction coefficient, anisotropic thermal parameters of all non-hydrogen atoms, and an isotropic thermal parameter for the hydrogen atom converged to $R_1 = 0.0222$ (on F) and $wR_2 = 0.0570$ (on F^2) for all data. The crystallographic data are summarized in Table 1. The atomic positional and isotropic thermal parameters and selected bond distances and angles are listed in Tables 2 and 3, respectively.

Solid State NMR Spectroscopic Studies. Proton magic angle spinning (MAS)[21,22] spectra were obtained with a Varian UNITYplus 300 instrument operating at 7.05 T. The corresponding Larmor frequency for proton was 300.08 MHz. The proton channel of the Varian variable temperature cross polarization (CP)[21] MAS probe with a 7 mm diameter silicon nitride rotor was employed. All spectra were taken at room temperature and with a spinning rate of 1.5−4.8 kHz, 1 μs pulse length, 3 s repetition delay, and 100 kHz spectral window. The 90° pulse length was 4.5 μs and the short flip angle (20°) rather than 90° was employed to excite the wide spectral window uniformly. The chemical shift was referenced to the external tetramethyl silane (TMS); the error range was within 1 ppm. Each spectrum was corrected for the background by running a blank sample.

The spectra were simulated with a homemade simulation program for MAS spectra based on the algorithm in the literature.[22,23] The input parameters necessary for the simulation were the three components of the principal chemical shift anisotropy (CSA) tensor, δ_{11}, δ_{22}, and δ_{33} ($\delta_{11} \le \delta_{22} \le \delta_{33}$) in ppm, the proton Larmor frequency of 300.08 MHz, and the spinning rate. The CSA here includes all CSA-like interactions, that is, not only the diamagnetic chemical shift anisotropy but also the ones described in the CSA tensor form such a Knight shift anisotropy or demagnetization interaction.

Vanadium static echo NMR experiment was attempted at 8.45 T with a Larmor frequency of 94.56 MHz. The echo pulse sequence of 1.63 μs pulse−30 μs delay−3.26 μs pulse was employed when the solution 90° pulse length was 6.52 μs. One MHz spectral width and 3 s repetition delay were employed.

Characterization. Thermogravimetric curve of $K(VO)(SeO_3)_2H$ was recorded on a Perkin-Elmer TGA-7 up to 600 °C with a heating rate of 10 °C/min under N_2 flow. A single step weight loss occurred at 350−530 °C of 60.8% which agreed well with the theoretical value, 61.8%, for the decomposition of $K(VO)(SeO_3)_2H$ into KVO_3.

A room temperature electron paramagnetic resonance (EPR) spectrum was obtained on a Bruker ER 031 X-band spectrometer with a frequency of 9.56 GHz. The magnetization data in the temperature range 5−300 K were obtained on a SQUID magnetometer with a magnetic field of 500 G. An infrared spectrum was recorded with a Nicolet 205 spectrometer with KBr pellet in the frequency range 400−4000 cm^{-1}.

Table 2. Atomic Coordinates ($\times 10^4$) and Equivalent Isotropic Displacement Parameters (Å$^2 \times 10^3$) for $K(VO)(SeO_3)_2H$

	x	y	z	$U_{eq}{}^a$
Se	1900(1)	5118(1)	2897(1)	10(1)
V	9434(1)	7500	520(3)	9(1)
K	5525(2)	2500	1010(4)	18(1)
O(1)	9512(6)	7500	4469(11)	16(1)
O(2)	1189(4)	6171(3)	−145(7)	14(1)
O(3)	2387(4)	3804(3)	713(8)	13(1)
O(4)	3890(4)	5749(3)	3818(8)	18(1)
H^b	5000	5000	5000	60(34)

^{a} $U_{eq} = {}^1/_3(U_{11} + U_{22} + U_{33})$. ^{b} This position may be an average of two split hydrogen atoms in an asymmetric hydrogen bonding or randomly distributed hydrogen atoms about the O(4)−O(4) axis (see text).

Table 3. Selected Bond Lengths (Å) and Angles (deg) for $K(VO)(SeO_3)_2H$

Se−O(4)	1.701(3)	V−O(1)	1.608(5)
Se−O(3)	1.702(3)	V−O(2) × 2	1.997(3)
Se−O(2)	1.706(3)	V−O(3) × 2	1.998(3)
K−O(4) × 2	2.765(4)	K−O(3) × 2	2.808(3)
K−O(4) × 2	2.792(3)	K−O(2) × 2	2.989(3)
O(4)−Se−O(3)	99.9(2)	O(1)−V−O(2) × 2	100.8(2)
O(4)−Se−O(2)	97.5(2)	O(1)−V−O(3) × 2	101.5(2)
O(3)−Se−O(2)	102.2(2)	O(2)−V−O(2)	87.9(2)
Se−O(2)−V	121.5(2)	O(2)−V−O(3) × 2	157.71(13)
Se−O(3)−V	118.9(2)	O(2)−V−O(3) × 2	88.88(12)
Se−O(4)−O(4)′ ^{a}	115.9(2)	O(3)−V−O(3)	85.8(2)

^{a} O(4)′ is hydrogen bonded to O(4).

(19) Sheldrick, G. M. *Acta Crystallogr*. **1990**, *A46*, 467.
(20) Sheldrick, G. M. SHELXL-93: A program for crystal structure determination, University of Gottingen, Germany, 1993.
(21) Mehring, M. *Principles of High Resolution NMR in Solids*, 2nd ed.; Springer-Verlag: Berlin, Heidelberg, Germany, New York, 1983.
(22) Herzfeld, J.; Berger, A. *J. Chem. Phys*. **1979**, *70*, 3300.
(23) Skibsted, J.; Nielsen, C. N.; Bildsoe, H.; Jakobsen, J. H. *Chem. Phys. Lett*. **1992**, *188*, 405.

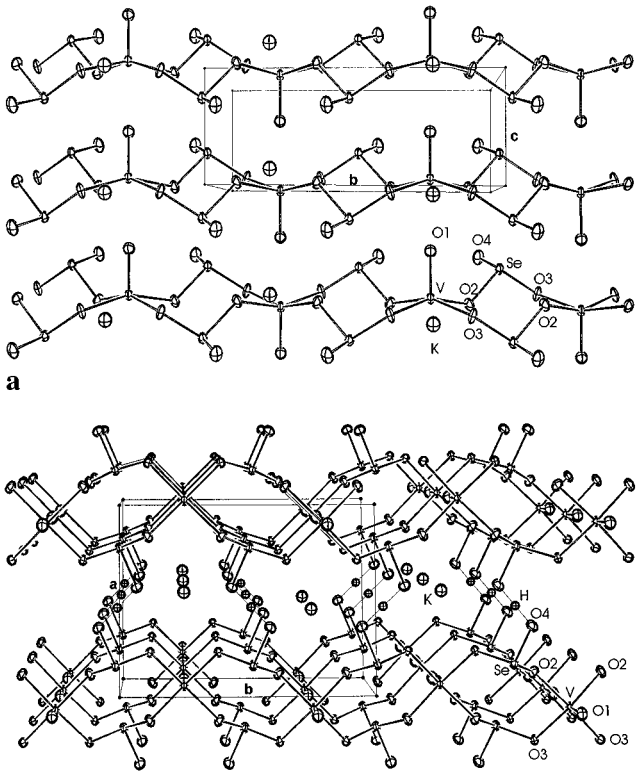

Figure 1. Structure of $K(VO)(SeO_3)_2H$ (a) viewed perpendicularly to the *bc*-plane and (b) perpendicularly to the *ab*-plane.

Results and Discussion

Synthesis. The title compound was first obtained as an impurity phase in the synthesis of KV_2SeO_7.[4] The reactions were run with V_2O_4, V_2O_5, SeO_2, and KOH in the mole ratio 3:1:15:10. In a similar fashion, green prism crystals of $K(VO)(SeO_3)_2H$ were obtained as a minor component of a mixture product from a hydrothermal reaction of V_2O_4, SeO_2, and KOH in a mole ratio of 1.5:15:5 (in millimoles) in 10 mL of distilled water. The majority of the mixture was unreacted V_2O_4 and KV_2SeO_7. The mole ratio has been varied in order to improve the yield and purity, but this was not successful. Typical yields of the desired $K(VO)(SeO_3)_2H$ phase were less than 10% by visual estimates.

Since V_2O_4 was recovered as the major phase in these reactions, we thought that its low solubility might be the cause of the low yield of $K(VO)(SeO_3)_2H$. Therefore, we have tried some reactions starting from soluble $VOSO_4$ instead of V_2O_4. From a reaction of $VOSO_4$:SeO_2:KOH = 3:15:3 the desired phase was obtained as pure microcrystals in much higher yield up to about 80% based on vanadium metal. The pH of the resultant solution was 0.7. Similar reactions with varied reagent ratios were tried in this system. When the final pH was higher than 1, there appeared significant amounts of impurity phases of unknown nature.

We have also tried to synthesize a Rb analogue of $K(VO)(SeO_3)_2H$. Indeed, in some reactions starting with V_2O_4, SeO_2, and RbOH, we could obtain a few green crystals. However, its yield and crystallinity were too low to do any further study. The difference in cation sizes of K and Rb may be responsible for the different synthesis results and crystallinity.

Crystal Structure. The crystal structure of $K(VO)(SeO_3)_2H$ is shown in Figure 1. The structure clearly shows chains composed of VO_5 square pyramid and SeO_3 trigonal pyramid units. The chain direction is the *b*-axis of the unit cell. Each vanadium atom is bonded to an apical oxygen and four SeO_3 units (through the basal oxygen atoms of the square pyramid) which are, in turn, bonded to the neighboring vanadium atoms in the same chain. The apical oxygens of the VO_5 square pyramids point up and down alternatively with respect to the *ab*-plane of the unit cell. The four basal oxygens, two O(2) and two O(3), have practically the same V−O distance of 1.997(3) (V−O(2)) and 1.998(3) Å (V−O(3)). Symmetry-related oxygens are arranged in cis configurations around the vanadium atom. The cis O−V−O bond angles for these oxygens are in the range 100.8(2)−101.5(2)°, indicating that the square pyramidal geometry is regular.

The apical oxygen (O(1)) has a V−O distance, 1.608(5) Å, which can be expressed as a V═O vanadyl group, typical for V(IV) oxo compounds. This oxygen is, in turn, weakly bonded to the vanadium atom of neighboring chain with a V−O distance of 2.481(5) Å to make an alternating V═O···V═O··· linkage along the *c*-direction (Figure 1a). This weak V···O bond will make the coordination environment of the vanadium a heavily distorted octahedron. A similar vanadium environment is found in the $VOSeO_3 \cdot H_2O$ structure.[3]

The terminal O(4) atoms of the selenite groups form interchain hydrogen bondings (Figure 1b). Evidences for the presence of a hydrogen atom will be given in the following sections. The short interchain O(4)−O(4) distance, 2.459(6) Å, is in the range of strong hydrogen-bonded O−O distances, 2.4−2.7 Å.[11] Without a hydrogen bonding between them, no two oxygen atoms can be closer to each other than 2.7 Å, the sum of their van der Waals radii. Infrared spectrum showed no absorption beyond 1000 cm^{-1}, an indication for strong hydrogen bonding.[15,16] Indeed, the difference Fourier map after the final cycle of the refinements including all non-hydrogen atoms revealed a peak of 0.67 $e^-/Å^3$ right in the middle of these two oxygens. Placing a hydrogen atom at this position would make the formula $K(VO)(SeO_3)_2H$ and the vanadium oxidation state +4. If this is the actual hydrogen atom position, this hydrogen bonding has two equal O−H bonds on both sides and the O−H−O bond angle is 180°. The same local O−H−O geometry was found in protonated *N*-nitrosopyrrolidine studied by single-crystal X-ray crystallography in which the inversion-related O−O distance was 2.47 Å and the hydrogen was at the inversion center.[13] However, the refined isotropic thermal parameter for the hydrogen atom in our crystal was rather large (see Table 2), indicating that this position may be an average of statistically distributed positions around this inversion center.

Certainly, the short O−O distance is not a guarantee for a symmetric hydrogen bonding. Reported neutron single-crystal structures with O−O distances in the range 2.4−2.5 Å show about half and half distribution between symmetric and asymmetric hydrogen bondings.[11] In fact, most of the crystal structures with symmetric hydrogen bondings have the hydrogen atoms at the inversion centers and the donor and acceptor atoms are inversion related. Whether this is an artifact due to the center of symmetry is not clear from the crystal structures alone.

On the other hand, various bonding models suggest that the symmetric hydrogen bondings are formed only if the O−O distances are extremely short, i.e., about 2.40 Å or even shorter.[11,12,18] Moreover, according to the compilation of crystal data on O−H−O hydrogen bondings, the discrimination between the symmetric and asymmetric bonding is also influenced by the nature of the atoms outside the hydrogen bondings.[18]

As a matter of fact, the foregoing discussion may be an oversimplification because the potential function for a hydrogen atom in the symmetric hydrogen-bonding changes continuously to that of the asymmetric one with increasing O−O distance and there is no clear-cut difference between the two.[12] Refine-

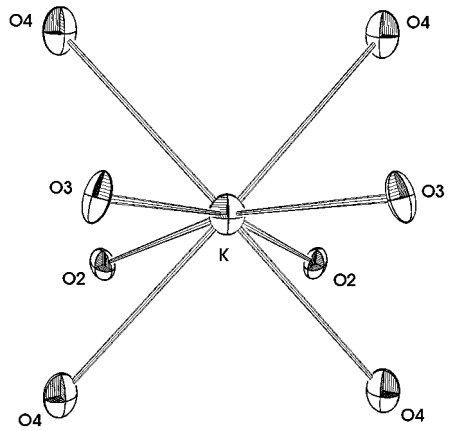

Figure 2. Oxygen environment for potassium atom in K(VO)(SeO$_3$)$_2$H.

ments of our crystal data in both symmetric and asymmetric models did not make any significant difference in terms of the final statistics. Since we cannot tell one from the other from the X-ray diffraction and the solid state NMR data (see below) suggest yet another possibility for the hydrogen position, we only list the (possibly) averaged position in Table 2.

Between the chains are the potassium atoms coordinated to eight oxygen atoms of the neighboring chains to balance the negative charges of the chains. The oxygen environment for the potassium atom is shown in Figure 2. The interchain interactions in this compound are 3-fold: first, the V═O···V═O interaction along the *c*-direction; second, Se−O−H−O−Se hydrogen bonding in the *b*-direction; third, and probably the strongest, the ionic interactions between the potassium atoms and the neighboring chains.

Solid State NMR Studies. Supporting evidences for the presence and nature of the hydrogen atom were obtained from solid state NMR studies for both ^{51}V and ^{1}H nuclei. There was no signal at all in the solid state ^{51}V NMR spectrum, consistent with the paramagnetism of a V(IV) nucleus.[24]

The protons are all magnetically equivalent which is evident from the single isotropic peak in the proton NMR spectrum. MAS spectra taken at several different spinning speeds (Figure 3) were employed to check the number of isotropic peaks and to reduce errors in obtaining CSA parameters. The isotropic peak position is independent on the spinning rate while spinning side bands occur at every interval of spinning rate from the isotropic peak over the range of a CSA pattern.[21] This observation suggests that the proton is located in a well-defined crystalline site in agreement with the crystallographic results. Simulations of the MAS spectra resulted in three CSA tensor components $\delta_{11} = -39$, $\delta_{22} = 2$, and $\delta_{33} = 94$ ppm. The isotropic chemical shift, $\delta_{iso} = 19 \pm 1$ ppm, and the asymmetry parameter, $\eta = 0.55$, were calculated from the three δ values according to the literature relationship.[25]

The δ_{iso} value of 19 ppm falls in the range of reported values of 16−20 ppm for strong hydrogen-bonded protons.[12,15] However, one has to be careful in comparing these values because most of the literature data are on organic molecules in solutions while ours is on an inorganic solid state compound with paramagnetic V(IV) nuclei which may influence the chemical shift. If paramagnetic effect on the NMR results is negligible, the nonzero asymmetry parameter can be interpreted due to noncylindrical symmetry for the proton. This seems to disagree with the picture derived from the X-ray crystal structure analysis,

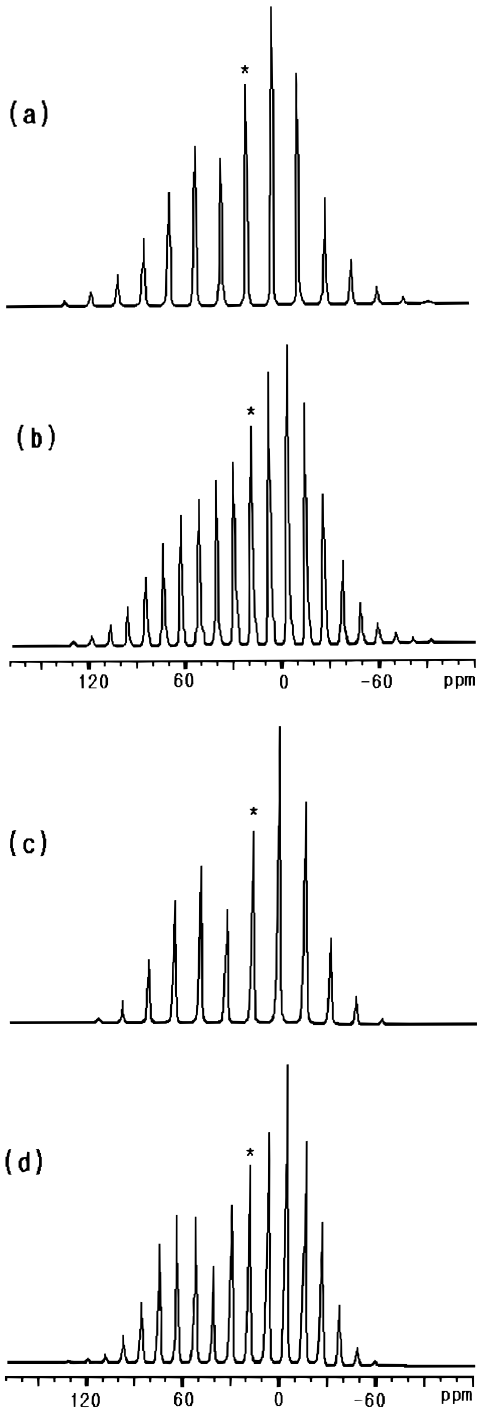

Figure 3. Experimental proton MAS NMR spectra of K(VO)(SeO$_3$)$_2$H taken at 7.05 T and at the spinning rate of (a) 4.83 kHz and (b) 3.35 kHz. Simulated proton MAS NMR spectra at the spinning rate of (c) 4.83 kHz and (d) 3.35 kHz. The peaks marked with * are isotropic peaks and the others are spinning side bands. See text for the input parameters.

that is, the O−H−O angle of 180°. The proton may reside off the O−O axis, and what we see in the crystal strucure is, in fact, an averaged electron density, giving another possibility for the O−H−O geometry. Alternatively, the nonzero asymmetry parameter is possibly due to the second nearest neighbors to the proton. Even if the O−H−O angle is 180°, the local symmetry of the proton deviates from the cylindrical symmetry when selenium and other neighboring atoms to the O−H−O bonds are taken into consideration.

The dipolar interaction between the nearest protons, expected to give at most about 1 kHz full width at half-height, was

(24) Harris, K. R., Mann, E. B., Eds. *NMR and the Periodic Table*; Academic Press: London, New York, San Francisco, CA, 1978.
(25) Duncan, T. M. *A Compilation of Chemical Shift Anisotropies*; The Farragut Press: Chicago, IL, 1990.

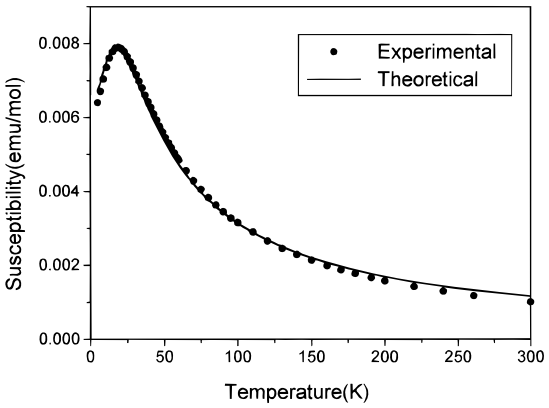

Figure 4. Magnetic susceptibility data vs temperature plot for K(VO)-$(SeO_3)_2H$. The experimental data are given as dots, and the theoretical fit to the 1D Heisenberg model for $S = {}^1/_2$ with $g = 1.97$ and $J/k = 13.8$ K is the solid line.

negligible compared with the about 40 kHz wide CSA interaction. The dipolar interactions with other nuclei such as oxygen and potassium are expected to be even smaller than that between protons due to their smaller magnetogyric ratios and natural abundance. The observed CSA width is at least three times broader than typical diamagnetic inorganic ones[25] probably due to demagnetization broadening resulting from the paramagnetic properties of the sample.[26] Although the observed δ_{iso} is in the range of reported values for protons in some diamagnetic inorganic materials,[25] the overall width of the CSA suggests the possibility of a paramagnetically shifted δ_{iso}. Therefore, the good fitting of our MAS spectra with a single set of CSA parameters indicates that the diamagnetic chemical shift interaction is negligible compared with paramagnetic interaction or their tensors happen to have the same principal axis system. Either case would not tell the exact location of hydrogen in the crystal. Only in the case that diamagnetic interaction is dominant as described in the previous paragraph or the paramagnetic and the diamagnetic interactions are different from each other only in magnitude, it is reasonable to deduce the hydrogen site.

Further NMR studies including magnetic field dependence study with separate measurement of magnetic susceptibility may give a definitive solution for the proton geometry.

Magnetic Properties. The magnetic susceptibility vs. temperature plot for $K(VO)(SeO_3)_2H$ is given in Figure 4. There is an antiferromagnetic coupling below ca. 19 K. The data $50 < T < 300$ K fit to the Curie−Weiss formula well with a Weiss temperature of −4.8 K and $C = 0.322$ K cm^3/mol which corresponds to $\mu_{eff} = 1.603\,\mu_B$. The effective magnetic moment falls in the typical range of $1.6-1.7\,\mu_B$ for a d^1 ion. Smaller values than the theoretical spin-only one ($1.73\,\mu_B$) is attributed to the spin−orbit coupling.[27] As the crystal structure implies, the antiferromagnetism must arise from superexchange interactions between the vanadium(IV) atoms within a chain mediated by the selenite double bridges. The distance between two vanadium atoms along the chain is 5.2149(4) Å, *b*/2, and this is too large a value to allow direct V−V interactions. The intervanadium distance of the V═O···V═O linkage is the same as the *c*-parameter, 4.0872(7) Å. However, in the magnetic study on $VOSeO_3 \cdot H_2O$, where exactly the same arrangement is present, contributions of such array to the magnetic coupling are found to be negligible.[3] The magnetic susceptibility curve was fitted to an 1D Heisenberg model for $S = 1/2$ (solid line in Figure 4).

$$\chi_m = \frac{N\mathbf{g}^2\mu_B^2}{kT}\,\frac{A + BX^{-1} + CX^{-2}}{1 + DX^{-1} + EX^{-2} + FX^{-3}} + \frac{G}{T}$$

where $X = kT/|J|$, **g** is the powder-averaged *g* factor, and *J* is the exchange constant. The first term is the formula from a 1D $S = {}^1/_2$ Heisenberg system; the constants $A = 0.25$, $B = 0.14995$, $C = 0.30094$, $D = 1.9862$, $E = 0.68854$, and $F = 6.0626$ calculated theoretically for this system were used.[28] The second term is a correction for paramagnetism that follows the Curie law. A good fit was obtained with $\mathbf{g} = 1.97$ and $J/k = 13.8$ K. The *g* value obtained from this fit agrees nicely with that calculated from the EPR spectrum, 1.969. The room temperature EPR spectrum shows a sharp singlet, indicating that there is only one magnetic species in this compound.

Conclusion. We have performed hydrothermal reactions in the V_2O_4, SeO_2, and KOH system to synthesize a new solid state compound $K(VO)(SeO_3)_2H$. The crystal structure of this compound shows one-dimensional chains of $[(VO)(SeO_3)_2]^{2-}$ that are linked to the next ones via three different mechanisms. The presence of hydrogen atoms is evidenced from a proton solid state NMR spectrum and X-ray single-crystal structure analysis. This proton constitutes a strong hydrogen bonding that holds the chains together although the exact nature of it is still in question. More experimental evidences are required to understand the nature of the hydrogen bonding. The magnetic V(IV) ions are coupled antiferromagnetically along the chain direction through the superexchange mechanism.

Acknowledgment. We thank Prof. H. Namgung of Kookmin University for the single-crystal X-ray data, Prof. Y-C. Park of Sung Kyun Kwan University for the EPR spectrum, and Dr. E. K. Jang and Mr. Y.-S. Kim of KBSI for the proton NMR simulation and for the SQUID operations, respectively. The financial support is from the KOSEF (Grant 951-0303-003-1).

Supporting Information Available: Tables of crystal data, anisotropic thermal parameters, and bond distances and angles for K(VO)-$(SeO_3)_2H$ (5 pages). Ordering information is given on any current masthead page.

IC960624Z

(26) (a) Stoll, M. E.; Majors, T. J. *Phys. Rev. B* **1981**, *24*, 2859. (b) Narath, A. In *Hyperfine Interactions*; Freeman, A. J., Trankel, R. B., Eds.: Academic Press: New York, 1967; Chapter 7.

(27) Banerjia, D. *Coordination Chemistry*; McGraw-Hill: Delhi, 1993; pp 211−214.

(28) Hatfield, W. E. *J. Appl. Phys.* **1981**, *52*, 1985.